Fluorescence Studies of Associating Polymers in Water: Determination of the Chain End Aggregation Number and a Model for the Association Process

Ahmad Yekta, Bai Xu, Jean Duhamel,[1] Hendra Adiwidjaja, and Mitchell A. Winnik*

Department of Chemistry and Erindale College, University of Toronto, Toronto, Ontario, Canada M5S 1A1

Received June 14, 1994; Revised Manuscript Received November 15, 1994®

ABSTRACT: Fluorescence probe experiments were carried out on aqueous solutions of urethane-coupled poly(ethylene oxide) polymers containing $C_{16}H_{33}O$ end groups. These HEUR polymers associate in water, giving rise to a sharp increase in zero-shear viscosity with increasing concentration above 0.2–0.5 wt % polymer and a pronounced shear thinning at modest shear rates. At very low concentrations (a few ppm), the hydrophobic end groups of these polymers come together to form micelle-like structures. We are interested in the mechanism of the polymer association and in determining the number of hydrophobic groups N_R that come together to form the micellar core. Fluorescence decay studies of pyrene excimer formation give values of N_R close to 20, independent of polymer concentration. This N_R value is a factor of 3 smaller than that found for typical nonionic micelles but larger than that inferred indirectly from different measurements on similar HEUR polymer systems. Steady-state fluorescence studies of intramolecular excimer formation in bis(1-pyrenyl)methyl ether (dipyme) solubilized in these polymers indicate that the micellar core is much more rigid than that of traditional surfactant micelles, with an estimated "microviscosity" an order of magnitude larger than that of sodium dodecyl sulfate micelles. A model is developed to accommodate these observations. In this model, the polymers form rosette-like micelles comprised of looped chains. At higher concentrations, larger structures are formed from aggregation of these micelles, held together by chains which bridge the micelles. The influence of dilution and of shear is to induce a bridge-to-loop transition, leading to a breakup of larger structures to smaller objects, micelles and smaller micelle aggregates.

Introduction

Many water-soluble polymers containing hydrophobic substituents undergo association in aqueous solution. Depending upon the microstructure of the polymer, the size of the hydrophobic groups, and their location in the polymer, this association can be either intramolecular, intermolecular, or both. Several types of these associating polymers have found application as rheology modifiers for coatings applications. Such polymers are often referred to as associative thickeners (AT's).[2,3] Among the characteristics of their solutions in water is high viscosity at relatively low polymer concentrations (i.e., 0.5–5 wt %) and a very rapid rise in the zero-shear viscosity with increasing concentrations. At higher shear rates there is often a transition region where the viscosity increases (shear thickening), followed by a dramatic drop of solution viscosity (shear thinning).[3] At the molecular level, the features of interest include the mechanism of association, including the association structure of the polymer in solution and the nature of the response of this structure to shear and elongational stresses, all as a function of polymer structure and the nature of the hydrophobe.

A well-known class of AT's are the (telechelic) urethane-coupled poly(ethylene oxide)s (PEO's) with hydrophobic end groups. These are often referred to as HEUR-type AT's. These materials are prepared by reacting a hydroxyl-end-capped PEO with a diisocyanate (DI) and an aliphatic alcohol (or an alkylphenol). One obtains a condensation polymer whose mean chain length depends upon the DI/PEO ratio.[4,5] These polymers have recently attracted widespread attention, in part because of their applications to paint and paper coatings technology, but also, because of their relatively well-defined structure, they serve as useful model polymers for molecular studies of the association process. One of the features of this type of polymer, which contains hydrophobic groups at the chain ends, is that in steady shear they exhibit Newtonian behavior up to relatively high shear rates. By contrast, polymers having associating groups distributed along the chain backbone tend to form gels that fracture under steady shear, or strongly shear thinning solutions, or solutions which undergo shear-induced gelation.[6]

Over the past few years, several major studies of the rheology of HEUR polymers in aqueous solution have been reported.[3,7–10] One of the most important findings from these experiments is that in oscillatory shear the data can be fitted to the simplest model of viscoelastic behavior, a Maxwell model consisting of a single elastic component connected in series with a single viscous element. This result implies that stress relaxation in these systems is characterized by a single relaxation time, which has been shown to depend upon the length of the hydrophobe as well as the concentration and molecular weight of the polymer.[9]

These experiments have been complemented by spectroscopic studies using either fluorescent probes[11–15] or, in one case, a HEUR polymer labeled with a pyrene-containing hydrophobe.[16] The spectroscopy experiments establish that polymer association in these systems arises through interactions among the hydrophobic substituents to create hydrophobic microdomains which have properties similar to those of nonionic micelles.

At elevated concentrations where the low-shear viscosity is high, the system may be viewed as a transient network of polymers bridging hydrophobic cores comprised of the hydrophobic groups. Annable et al.[9] carried out extensive steady-shear and oscillatory shear experiments on a series of HEUR polymers with differ-

® Abstract published in *Advance ACS Abstracts,* February 1, 1995.

0024-9297/95/2228-0956$09.00/0

ent end groups. They interpreted their rheology data in terms of the transient network model of Tanaka and Edwards[19] and associated the relaxation time obtained from each oscillatory shear experiment to the time needed for a hydrophobe to exit from a micelle core within the network. To accommodate the concentration and molecular weight dependence of the viscoelastic behavior, they had to modify the model to include topological considerations: micelle-like objects at lower concentrations that associated into larger structures held together by bridging chains at higher concentrations, with a concentration-dependent competition between looping and bridging within the network.

Hansen and co-workers[8,17,20] examined the dynamic processes of the associated structures by a combination of dynamic light scattering (DLS) and pulsed-gradient spin–echo ^{1}H NMR (PGSE) experiments. These experiments show a crossover from classical Fickian diffusion at relatively low concentrations to anomalous diffusion at concentrations where the zero-shear viscosity mounts.[20] Here they find a distribution of relaxation times which can be described in terms of the mode-coupling theory developed by Ngai.[20c]

Spectroscopy measurements indicate that the onset of association in these systems normally occurs at concentrations more than an order of magnitude lower than that probed by viscosity or polymer diffusion experiments.[11–16] In this concentration region, one must have polymer association which occurs in such a way that it makes only modest contributions to the solution viscosity. Various views have been put forward about the nature of that association. Many of these views have been based on the idea that the number of hydrocarbon chains which associate to form the micellar core is small,[3,15–17] with $N_R < 10$.

Small N_R values have been inferred, for example, from the fitting of viscoelastic response data to classical rubber elasticity models.[3,9] Maechling-Strasser et al. propose an open association model in which both the aggregation number for hydrophobe association and the total molar mass of the associated polymer structure increase with polymer concentration.[15a] Their evidence in support of this model was that the apparent weight-averaged molecular weight of the polymer in aqueous solution, as measured by light scattering, increased with polymer concentration over the concentration range of 0.1–2.0 wt %. Hansen and co-workers interpreted their diffusion measurements in terms of very small aggregation numbers (i.e., 2–5) for the polymer chain ends. They commented that if the aggregation number is really this small, i.e., $N_R < 10$, one might question whether the micelle concept applies at all for systems of this kind.[17] From another point of view, lattice-based Monte Carlo simulations of chains with sticky ends as a model of transient association also led to the idea of only a few interacting chain ends per associated unit.[18]

We have proposed a very different model for the association process, based upon our preliminary finding, with two HEUR polymers bearing $C_{16}H_{33}O$ end groups, that the number of hydrocarbon chains that associate to form a micellar core was close to 20 and independent of polymer concentration.[14] On this basis, we proposed that over the concentration range of ca. 10 ppm to 0.4 wt %, our HEUR polymers were present predominantly in the form of "rosette"-like micelles. We further suggested that these species were composed of 10 polymer chains all cyclized to form a micellar core containing 20 end groups, i.e., $N_R = 20$, and that at higher concentrations a loop-to-bridging transition occurs without perturbing the magnitude of N_R. This is a closed association model in which the core size and the micelle size are independent of polymer concentration.

As the concentration of polymer in the system is increased, larger objects do form. These are seen as micellar aggregates or clusters of micelles held together by bridging chains. Our model is pictorially similar to that proposed independently by Annable in the context of the rheology measurements described above.[9] A key feature of this model is that over a range of concentrations just above the onset of end group association, the system is comprised largely of individual micelles composed of looped chains. In support of this idea, we note that Fonnum et al.[7a,8] have carried out osmometry experiments on several HEUR polymers in aqueous solution. In the "dilute" solution limit, they found apparent molecular weights suggesting the association of 18 polymer chains per aggregating cluster. If this object is a single micelle with all its chain ends located within the core and all chains have two hydrophobe end groups, it would have $N_R = 36$.

One of the functions of this paper is to report in detail the experiments on which our model is based. We examine the properties of five HEUR polymers prepared by the reaction of PEO with isophorone diisocyanate (IPDI), four of which contain $C_{16}H_{33}O$ groups as the terminal hydrophobic groups. The nominal chemical structures of these polymers are given below. Two of these samples were among those whose viscoelastic properties were studied by Jenkins, and the sample numbers **22-2** and **22-3** are the same as those noted in his thesis.[3] Sample **AT 107** and its deuterated analogue ($C_{16}D_{33}O$ end groups) were prepared by Jenkins at Union Carbide.

$C_{16}H_{33}O$-IPDU-[PEO-IPDU]$_y$-$OC_{16}H_{33}$

AT 22-2 (M_n = 34,000, M_w/M_n = 1.7, y = 4, PEO = 8,200)

AT 22-3 (M_n = 51,000, M_w/M_n = 1.7, y = 6, PEO = 8,200)

AT 107 (M_n = 26,800, M_w/M_n = 1.7, y = 3, PEO = 8,200)

AT 67-3 (M_n = 36,000, M_w/M_n = 1.1, y = 1, PEO = 35,000)

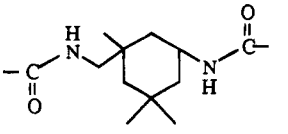

IPDU

Because of the way in which polymers **AT 22-2**, **22-3**, and **107** are prepared and because of difficulties in the synthesis of **AT 67-3**, these polymers contain fewer than two hydrophobic end groups per chain. These polymers are compared with a control polymer which has a structure very similar to that of **AT 22-2** but lacks the hydrophobic end groups. The control polymer is prepared by quenching the condensation polymer with water instead of $C_{16}H_{33}OH$. Although the structure of the polymer is frequently written as shown below with X = OH, the actual end groups on each chain end will depend upon whether that chain end prior to hydrolysis was a free PEO or an isocyanate from IPDI.

X-IPDU-[PEO-IPDU]$_y$-X

Control 23-2 (M_n = 34,000, M_w/M_n = 1.7, y = 4, PEO = 8,200)

Our major interest in this paper is the issue of the number of hydrophobic end groups (N_R) which associate

to form the micelle-like structures in the HEUR solutions. Our approach is to examine very carefully the kinetics of excimer formation for pyrene added as a fluorescent probe to solutions of these AT's in water. In addition, we use other fluorescent probes to gain further information about the local size and structure of the micellar core formed by association of the end groups.

Experimental Section

Materials. The polymeric associative thickeners **AT 22-2**, **AT 22-3**, **AT 107**, and **AT 67-3** are generous donations of Union Carbide (sample nos. 46RCHX22-2, 46RCHX23-2, and 6RDJY-107) and of Applied Biosystems (SMM9267-3-2), respectively. **AT 107** was prepared in the same way as the deuterated analogue employed by Ottewill et al. in small-angle neutron scattering studies.[21] **Control 23-2** (Union Carbide, 46RCHX23-2) is not a thickener. It has the same structure as **AT 22-2** without the hydrophobic end groups. In purification we take advantage of the temperature-dependent solubility of PEO in methanol (−15 °C, rapid precipitation) or ethyl acetate (10 °C, slow, overnight storage). A typical procedure is to dissolve the sample in the warm solvent (45 °C, 5 wt %) and cool to the appropriate temperature to precipitate (recrystallize) the PEO-based polymer but not the small-molecule contaminants. With ethyl acetate as the solvent, the procedure is simpler and filtration at room temperature is adequate. The above procedure was repeated three times. The last traces of solvent were removed from the sample by dissolution (10 wt %) in benzene followed by freeze-drying. Pyrene (Aldrich) was recrystallized three times from ethanol, followed by sublimation. Sodium dodecyl sulfate (SDS), 2-methylphenanthrene (McPhe), and 9-methylanthracene (MeAn) (all from Aldrich) were used as received. Bis(1-pyrenyl)methyl ether ("dipyme") was the sample reported previously.[22a,b] All solvents were from Caledon and of Spectroquality grade. Distilled water was further purified through a Millipore Milli Q purification system.

NMR Characterization of AT Polymers. ^{1}H NMR spectra were run on a Varian 500 MHz spectrometer using solutions containing 1−3 wt % of polymer and ca. 1 mM *p*-difluorobenzene in $CDCl_3$. To obtain quantitative integration of the signals, a pulse delay time of 20 s was found to be necessary for all of the systems under study. In most cases, 30−100 pulses were averaged.

Details of this characterization method will be published elsewhere.[22c] Here we summarize our findings. It is now well established that the synthetic procedures used to prepare many HEUR associative polymers leaves some of the PEO unreacted.[23] The information we seek from an ^{1}H NMR analysis is the number of moles of alkyl group per gram of polymer. In the region of 0.70−1.90 ppm of the ^{1}H NMR spectra of these polymers, there is significant overlap of the proton resonances of the *n*-alkyl (R) and the isophorone diurethane (IPDU) moieties. By appropriate synthesis of the two model compounds IPDU(OCH_3)$_2$ and IPDU($OC_{16}H_{33}$)$_2$, we determined that in the region of 0.70−1.10 ppm, IPDU contributes 12H, while the alkyl $C_{16}H_{33}$ contributes 3H. Also, we find that in the region of 1.10−1.90 ppm, IPDU contributes 3H, while each $C_{16}H_{33}$ group contributes 28H. It follows that the integration ($I_{(ppm)}$) of the NMR signals in the two regions can be written as

$$I_{(0.70-1.10)} = 12(\text{IPDU}) + 3(\text{R}) \quad (1)$$

$$I_{(1.10-1.90)} = 3(\text{IPDU}) + 28(\text{R}) \quad (2)$$

An algebraic solution of the two equations yields the *relative* molar contents of the alkyl R and of the IPDU linkages in the polymer. An internal standard, *p*-difluorobenzene, allows us to determine the absolute molar contents of R and IPDU. The latter compound has its ^{1}H NMR resonances (a triplet centered at 6.99 ppm) far away from those of the polymeric samples so that relative integrations are easily evaluated. In some samples, a peak due to traces of water appears in the range of 1.5−2.5 ppm. This signal interferes with proper integration of the relevant peaks. In this case, one employs eq 3 instead of eq 2 to analyze the spectrum.

$$I_{(1.10-1.40)} = (\text{IPDU}) + 26(\text{R}) \quad (3)$$

Saturation Experiments with Fluorescent Probes. Details of saturation experiments with pyrene were reported previously.[13] In these experiments, an aqueous solution of the polymer is exposed to excess dye, which is then removed after the system comes to equilibrium. Aqueous polymer solutions saturated with MePhe and MeAn (and also mixtures of the two substances) were prepared from 1.5 mM solutions of the dyes in cyclohexane. An aliquot was placed in a centrifuge tube, followed by evaporation of the solvent (N_2 flow, 40 °C). Then the AT solution ($C_{polymer}$ = 0.2−1.0 wt %) was added, stirred for 5−6 days, and centrifuged to remove excess chromophore.

Dissolution of dipyme is difficult and involves special procedures.[22b] Crystalline dipyme is very slow to dissolve in aqueous AT solutions. Stock 1 mM solutions of dipyme in acetone were injected directly into the stirred AT solution (1 μL/mL) to give solutions containing 1 μM dye. Immediately after the injection, microcrystals of dipyme form. These have their own characteristic excimer emission, which interferes with the study. The slow disappearance of the microcrystals is best studied by examining excitation spectra, which for the microcrystals is distinctly different at λ_{em} = 480 nm (cf. Figure 6a,b) than for dipyme monomer emission observed at 375 nm (cf. Figure 6c). When dipyme is completely dissolved, identical excitation spectra are obtained at both wavelengths. Complete dissolution of dipyme into the AT solution takes place over 4−5 days of continued stirring at room temperature. Similar experiments with injection of dipyme into pure water or 10 g/L aqueous solution of the control polymer (**Control 23-2**, same structure as **AT 22-2** but lacking the hydrophobic end groups) showed that no significant amounts of dipyme dissolved even after 2 weeks of continued stirring. These results show that the PEO backbone and the adjoining IPDU linkages do not solubilize dipyme in water. Concern over possible effects of the coinjected acetone was alleviated when a 10-fold increase in the quantity of injected acetone did not change our final results. It should be stressed that aerated solutions of dipyme are very liable to photooxygenation and should be protected from room light and extensive periods of irradiation.

UV Absorption Measurements. A Hewlett-Packard 8452A diode-array (2 nm resolution) or a dual-beam Perkin-Elmer λ6 (0.25 nm resolution) spectrophotometer was used. MePhe has a rather sharp absorption band (~3 nm bandwidth) at 297 nm and the instrument with higher resolution was needed. Extinction coefficients ϵ for the micellized (10 g/L AT) fluorescent probes were determined. These are pyrene (338 nm, 3.58×10^4 M^{-1} cm^{-1}), MeAn (390 nm, 1.07×10^4 M^{-1} cm^{-1}), and MePhe (297 nm, 8.40×10^3 M^{-1} cm^{-1}). In pure water, the solubilities are lower, and the absorption bands are blue shifted by ca. 2−3 nm. We obtain the following: pyrene (solubility 0.7 μM, $\epsilon_{335} \approx 1.7 \times 10^4$ M^{-1} cm^{-1}); MeAn (solubility 1 μM, $\epsilon_{387} \approx 1 \times 10^4$ M^{-1} cm^{-1}); MePhe (solubility 9.3 μM, $\epsilon_{295} = 4.8 \times 10^3$ M^{-1} cm^{-1}).

Rheology Measurements. A Rheometrics RAA2 analyzer equipped with a ϕ = 50 mm cone and plate was used in steady-shear and oscillatory shear measurement at 20 °C. The results are fitted into a single Maxwell element consisting of a serial connection of a spring and a dashpot.

Fluorescence Emission Measurements. A SPEX Fluorolog spectrometer was used and the conditions are those described previously.[13] All samples were aerated (temperature controlled at 20 ± 0.5 °C), magnetically stirred, and examined at a right-angle optical geometry. With the 10 g/L solution of AT, efficient stirring was not possible. Shear forces arising from various stirring rates or repeated cycles of heating (to 50 °C) and cooling (to 20 °C) had no observable effect on the intensity or the shape of the spectra.

Fluorescence Decay Measurements. Fluorescence decay profiles were measured by the single-photon-timing technique using instrumentation described previously.[24] The

excitation wavelength (λ_{ex}) for pyrene was 338 nm, and emission (λ_{em}) was observed at 376 nm (monomer emission) and also 520 nm (excimer emission). For MePhe, λ_{ex} was 297 nm, and λ_{em} was 350 nm. Reference decay curves of degassed solutions of 2,5-diphenyloxazole (PPO) in cyclohexane ($\tau = 1.33$ ns) were used to follow the excitation lamp profile. Most experiments had a maximum count of ca. 20 000.

Analysis of Pyrene Monomer Fluorescence Decays. For dilute (<1 μM) aerated solutions of pyrene in aqueous AT, one expects single-exponential decays. Single-exponential fits of observed decays yield a lifetime τ° of 250 ns (deoxygenated solutions yield $\tau^\circ = 360$ ns) with $\chi^2 = 1.3$. In the decay profile, there is an initially short-lived component that cannot be exclusively attributed to emission from the water phase. τ_w for pyrene in aerated water is 150 ns. However, the partitioning data[13] indicate that less than 1–5% of pyrene is in the water phase. Furthermore, an even smaller fraction of excitation light is absorbed by the pyrene in water because the samples are excited at 338 nm while the peak absorbance of pyrene in water is at 334 nm. We assign this short lived component of decay to a combination of residual excimer formation dynamics, heterogeneous quenching by oxygen dissolved in the medium, and Poisson-type quenching by residual impurities present in the polymer. Simulation of decay forms and fits to the micelle model convince us that a χ^2 of 1.3 affords us with a workable system for recovering the micellar aggregation numbers with an accuracy of ca. 5%.

For higher pyrene concentrations, the resulting nonexponential decays are fit to the micelle model, eq 4.[25] The model assumes a negligible rate for the dissociation of the excimer back to the excited monomer.

$$I(t) = I(0)\exp\left\{-\frac{t}{\tau^\circ} - n[1 - \exp(-k_1 t)]\right\} \qquad (4)$$

In this expression, there are four fitting parameters: the initial intensity $I(0)$, the unquenched lifetime τ°, the mean number of pyrene molecules per micelle n, and the first-order rate constant for the self-quenching of an excited pyrene by a ground-state pyrene molecule inside a micelle k_1. When the data are fit to a free variation of the four fitting parameters, we obtain χ^2 values in the range of 1.1–1.5, $\tau^\circ = 230$–270 ns, and the extracted values of n have a reproducibility of ±15%. However, substantial improvement is obtained if in the fitting procedure we add a small component of scattered light and fix the τ° value at 250 ns (determined independently at low pyrene concentration), with the result that the extracted n values have a reproducibility better than 5%. The reproducibility of k_1 values is not very sensitive to this procedure and remains about ±20%. Our initial data for the AT solutions gave k_1 values an order of magnitude lower than that found for micellar systems such as SDS. Considering the relatively small aggregation numbers we were recovering, the small value of k_1 was unexpected. As a consequence, we carried out extensive simulations of fluorescence decay profiles for micelle-forming systems with similar parameters. Confidence was gained in the faithfulness of the fitting procedure when we recovered parameters from the simulated data within ±2% of the input values.

Results and Discussion

Polymer Characterization. Before we embark on a discussion of the fluorescence results and how we obtain micellar aggregation numbers, it is important that we understand the structural characterization of our HEUR polymers. Fluorescence methods to determine aggregation numbers count the number of moles of micelles in the sample under study. In order to know the true value of N_R, one also needs to know the number of moles of alkyl hydrophobic groups participating in micelle formation. Of course, if the actual structure of the polymer is identical to the nominal structure given for the AT polymers, one can calculate the moles of R as twice the sample mass divided by the polymer molecular weight (M_n). However, our ^{1}H NMR results, together with work from other research groups, show that most telechelic AT's have fewer than the two expected hydrophobic groups per chain.[22c,23] We also find that when the samples are suitably purified,[26] the ^{1}H NMR spectra provide us with the required knowledge of the moles of R per gram of AT, independent of a knowledge of the polymer M_n value. The results are summarized in Table 1. The dramatic drop in end-group concentration [R] after purification suggests that we have removed some low molecular weight species from the reaction mixture. One likely component removed may be dihexadecyl IPDU.

Table 1. NMR Characterization of AT Samples

sample	q_{IPDU}[a]	q_R[a]	q_{PEG}[a]	mol wt (M_n)	alkyl groups per AT chain
AT 22-2					
purified	139	42.6	111	34 000	1.4
as received	136	56.0	110	34 000	
AT 22-3					
purified	147	33.3	132	51 000	1.7
as received	158	45.6	132	51 000	
AT67-3					
purified	24.9	26.5		36 000	0.96
6RDJY107					
purified	138	50	120	26 800	1.3
as received	160	77	120	26 800	

[a] q_{IPDU}, q_R, and q_{PEG} are contents of IPDU, R, and PEG in each polymer (the units are μmol/g of AT).

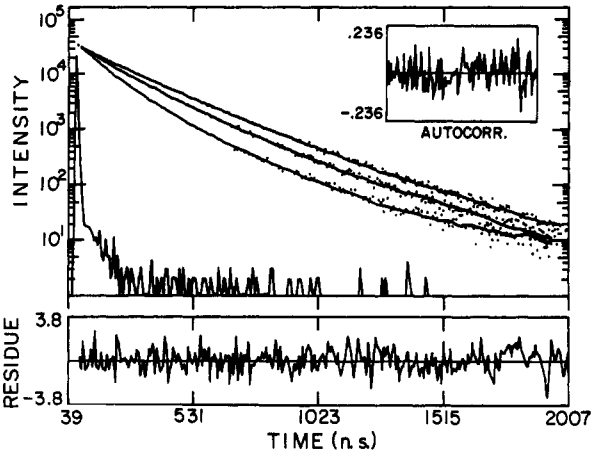

Figure 1. Fluorescence decay curves for pyrene solubilized in aqueous solutions of **AT 22-2** (1.0 wt %). The molar pyrene concentrations corresponding to each curve (top to bottom) are 20, 45, and 60 μM.

Fluorescence Quenching Experiments and Aggregation Numbers. Applicability of the Micellar Quenching Model. In dealing with the kind of complex micellar system expected for aqueous polymeric associative thickeners, one must ascertain that the data and the mathematical equations chosen to represent the system under measurement behave as expected. With τ° known independently, eq 4 contains three fitting parameters. Many nonexponential fluorescence decay profiles can be fitted successfully to an equation such as eq 4 with several parameters. In such cases, the goodness-of-fit (i.e., χ^2) does not in itself provide justification for the model. We seek confidence in the choice of our model through checking for the expected variation of the fitting parameters with our actual experimental variables. Figure 1 shows typical data for the fluorescence decays of pyrene monomer solubilized in aqueous AT. At higher Py loadings, the decays are markedly nonexponential. We fit the data to eq 4 and extract the

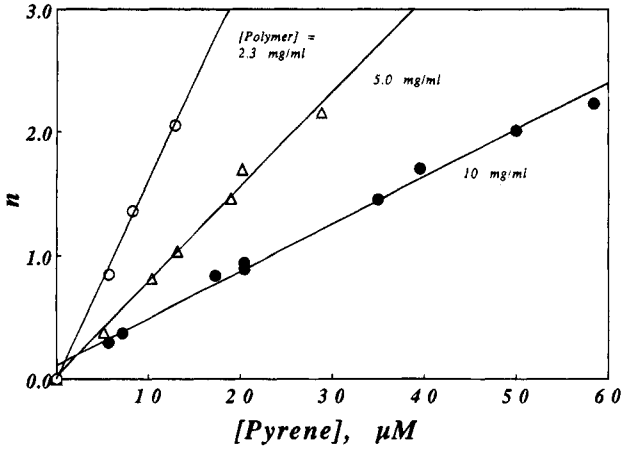

Figure 2. Plots of n vs pyrene concentration in aqueous solutions of **AT 22-2** for values of n obtained at different polymer concentrations.

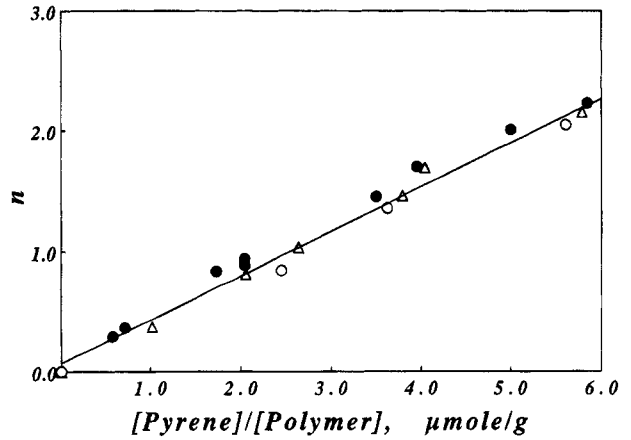

Figure 3. Data from Figure 2 plotted as n vs the amount of pyrene present per gram of polymer in solution.

two parameters n and k_1. The mean number of pyrene molecules per micelle is given by

$$n = \frac{[\text{Py}]}{[\text{Micelle}]} = \frac{[\text{Py}]}{C_{\text{polymer}}} \frac{N_R}{q_R} \tag{5}$$

Where [Py] is the pyrene concentration in moles per liter, C_{polymer} is the AT concentration in grams per liter, N_R is the aggregation number, and q_R is the alkyl chain content in the polymer (moles of alkyl per gram of polymer). In writing eq 5, we have neglected the critical micelle concentration term (cmc) because our earlier data show that the cmc is much lower than the AT concentrations we work with here.[13]

Equation 5 requires n to vary linearly with the [Py] loading. Figure 2 shows that for all concentrations of **AT 22-2** studied, eq 5 is obeyed. According to eq 5, if N_R is independent of C_{polymer}, then one should observe a universal linear dependence of n on the ratio [Py]/C_{polymer}. Figure 3 reveals that the various data sets of Figure 2 combine to give this universal behavior. These data imply that the micelle aggregation number does not change with increasing AT concentration.

The reaction between two pyrene molecules inside a micelle can be described by the expression

$$\text{Py}^* + \text{Py} \xrightarrow[\text{micelle}]{k_1} \text{excimer}^* \tag{6}$$

The simple quenching model that leads to eq 4 also predicts the pseudo-first-order rate constant describing this reaction (k_1) to be independent of [Py] and C_{polymer}. Figure 4 shows the data for k_1 obtained for sample **22-2**. Within the error limits involved, k_1 behaves as expected. In this way, we believe that we have established the validity of the Poisson quenching model used in our data analysis. Essentially identical values of k_1 were obtained for all four AT polymer samples over a similar range of polymer concentrations.

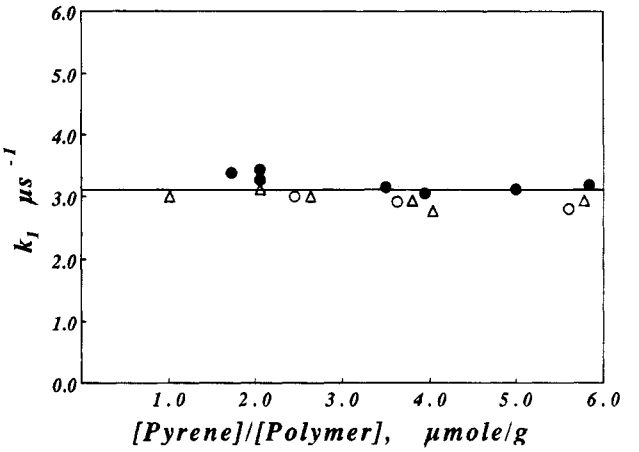

Figure 4. Values of k_1 obtained from the various experiments reported here plotted vs the amount of pyrene present per gram of polymer in solution.

Table 2. Aggregation Numbers of the Purified AT Polymers

	AT 22-2	AT 22-3	AT 67-3	AT 107
N_R	18	21	28	28
end groups per AT chain	1.4	1.7	0.96	1.3

Micellar Aggregation Number, N_R. Before we discuss our results, a few words about semantics are in order. This quantity is defined differently by various workers studying AT systems. Some workers have defined the aggregation number as the mean number of aggregating polymer chains per hydrophobic cluster. Others use the term to indicate the mean number of hydrophobic groups per micellar core, and we use the notation N_R to emphasize the reference to numbers of hydrophobic units. There are three reasons why we prefer this definition. First, this is how aggregation number is defined for surfactant micelle systems. Second, when N_R is defined in this way, one can compare results for various polymers with different numbers of alkyl substituents per chain. Third, and most important, with N_R defined in this way, transitions in the system which conserve the number of locally associated hydrophobic groups, such as the interconversion of bridged chains and looped chains among aggregates of micelles, also preserve the value of N_R.

Aggregation numbers are calculated from the slope of the line in Figure 3 using eq 5 and our knowledge of the hydrophobe content of the purified polymer. In this way we obtain $N_R = 18$ for **AT 22-2**, independent of AT concentration. (Without the ^{1}H NMR correction we would have calculated $N_R = 22$.) Similarly, for **AT 67-3**, we obtain $N_R = 28$. (Here, without the ^{1}H NMR correction we would have calculated $N_R = 59$, a very significant change.) The values of N_R for all four AT polymers are summarized in Table 2.

To summarize, the essential features of our data are as follows: (a) In the range of polymer concentration we examine, the macroscopic low-shear viscosity (η_0) of

the polymer solutions varies over about 2 orders of magnitude. In the most dilute solutions, $\eta_0 \approx \eta_{H_2O}$. However, even in these dilute solutions, the micelles remain intact and have the same core size as in the more concentrated and viscous solutions ($\eta_0 \approx 200$ cP). (b) N_R is not a small single-digit number as some authors have claimed. Neither is N_R as large as that observed for fully compact surfactant micellar systems[27] ($N_R \approx 50-70$). (c) The values of N_R for the four polymers vary from 18 to 27. These differences are larger than the statistical error in the fluorescence decay analysis, estimated at ±5%. They do depend sensitively on the end-group analysis for the polymers. Here the precision is also estimated at ±5%. Since there is no apparent pattern to the differences, we would prefer at this point to consider that the polymers have essentially identical values of $N_R \approx 20$. As a final comment, we note once again that all samples contain a large fraction of singly substituted alkyl chains which might affect micellar properties by virtue of their freely dangling ends.

Micelle Rigidity. The data of Figure 4 shows that, independent of polymer concentration, the rate constant $k_1 = 3 \times 10^6$ s^{-1}. Essentially identical values are obtained for all four AT systems. Given that N_R is three fold smaller than for SDS micelles, it is surprising that k_1 is one order of magnitude smaller than in SDS.[28] In homogeneous fluid media, the excimer formation rate is second order and essentially diffusion-controlled.[29] In micellar systems, one can also expect an encounter-limited rate. One can take $(1/k_1)$ as a measure of the mean time of encounter between two pyrene molecules inside a micelle. In the AT micelle the encounter time is 300 ns, while in SDS micelles, the value is 30 ns.

Micelle rigidity helps to explain why the Rohm and Haas group[16] calculated very small aggregation numbers in their HEUR AT polymers in which toluene diurethane coupled pyrenylbutyloxy groups to the PEO polymer. They prepared mixtures of labeled and unlabeled polymers and observed the extent of excimer formation by steady-state fluorescence measurements as a function of the composition of the mixture. Among the various assumptions they made in analyzing their data, the most serious was that a micellar core containing two pyrenes will always lead to excimer emission. This assumption is not so bad for very fluid structures. For microviscous environments, this will lead to a significant underestimation of the aggregation number.

In the pseudophase model of micelle structure, the hydrophobic portion is viewed as a collection of liquid droplets surrounded by the polar headgroups of the surfactant constituents. In ionic micelles, the headgroups are relatively small in size, and thus the radius of the micelle and that of the hydrocarbon "droplet" are comparable. In nonionic micelles, the polar portion is a water-soluble polymer, typically a PEO chain, which forms a water-swollen corona around the hydrophobic core. The core size depends upon the size of the hydrophobe and the aggregation number of the micelle, and the demarcation between the hydrophobic core and the hydrophilic corona is not well understood. From the point of view of the liquid droplet model, two factors can affect the rate of intradroplet excimer formation: the size of the droplet, which affects the local concentration, and the local fluidity (i.e., the local microscopic friction coefficient or "microviscosity"), which affects the rate of pyrene diffusion.

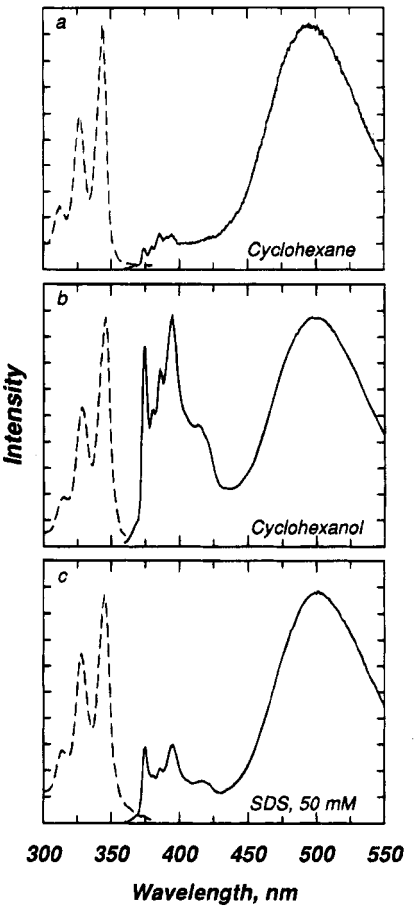

Figure 5. Normalized fluorescence emission and excitation spectra of dipyme at very low concentrations (1 μM) in cyclohexane, in cyclohexanol, and in an aqueous solution (50 mM) of SDS.

Scheme 1

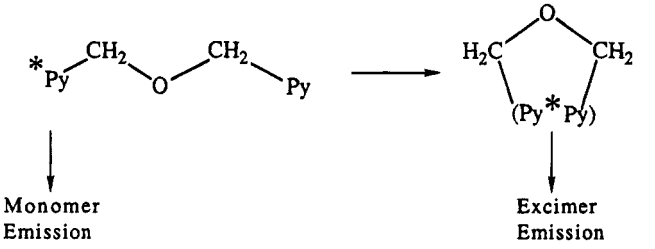

Micelle Rigidity and Estimating the Size of the Hydrophobic Core. Microviscosity in micellar systems is commonly probed by means of a fluorescence measurement sensitive to the local friction coefficient. One approach involves fluorescence depolarization measurements of molecules such as perylene, which measures the rotational diffusion of the probe.[30] Alternatively, one can examine the rate of conformational change in a bichromophoric molecule such as dipyme.[31] We prefer this approach here because the type of conformational change leading to excimer formation approximates the motion of pyrene diffusion to form an excimer in the micelle.

Dipyme as a Probe of Microscopic Viscosity.[21] Scheme 1 depicts the process of intramolecular cyclization and excimer formation of dipyme. The rate of this process is resisted by the local friction of its microenvironment. As an example, in Figure 5 we present the fluorescence spectra of dipyme in cyclohexane (viscosity $\eta = 0.66$ cP), cyclohexanol, a solvent some 2 orders of magnitude more viscous ($\eta = 65$ cP), and aqueous 0.05

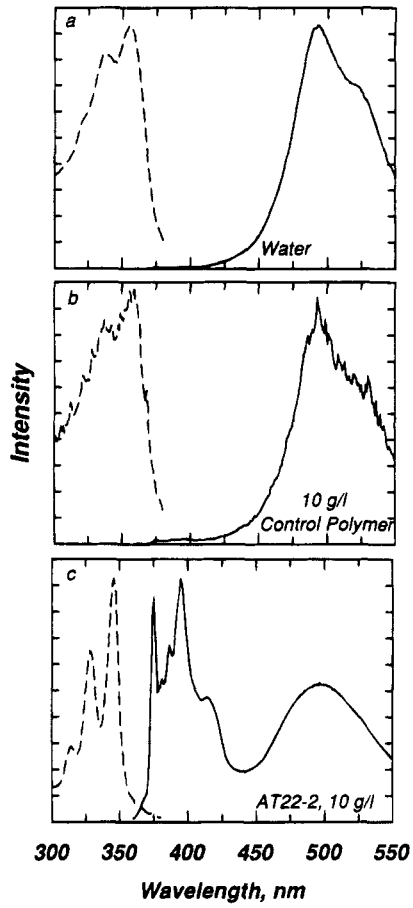

Figure 6. Normalized fluorescence emission and excitation spectra of dipyme at very low concentrations (1 μM) in water, in an aqueous solution (1 wt %) of the polymer **Control 22-3**, and in a corresponding solution (1 wt %) of **AT 22-2**. The upper two spectra correspond to those of dipyme microcrystals suspended in the medium.

M SDS. We notice that in the more fluid solvent we have enhanced excimer emission intensity.

Qualitatively, one sees that the dipyme fluorescence reports a microviscosity of the SDS micelles intermediate in value between the bulk viscosities of cyclohexane and cyclohexanol. Based upon more extensive comparisons with other solvents, various research groups have reported microviscosities of SDS micelles on the order of 20 cP.[31] One has to be careful not to overinterpret this value. Viscosity is a macroscopic quantity that becomes ill-defined on a microscopic scale, where, in fact, friction coefficients become a more appropriate measure of molecular mobility. In addition, the liquid droplet model ignores the detailed structure of the micelle, and probes located in different environments will sample different aspects of the structure. Finally, a probe may perturb its immediate environment (through dipolar interactions, H-bonding, etc.), and hence affect the frictional forces it experiences. On the other hand, there is rather widespread evidence that solubilization of these probes by normal micelles does not change their aggregation numbers.

Notwithstanding the above objections, we can compare the frictional forces dipyme experiences in various systems with that in the micellar AT solutions. Dipyme is insoluble in water and is not solubilized in water by the polymer (**Control 23-2**) lacking hydrophobic end groups. Fluorescence spectra obtained for these solutions (Figure 6a,b) are dominated by the presence of microcrystals of the probe which do not dissolve. Dipyme

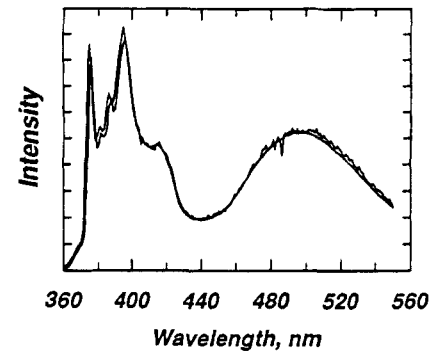

Figure 7. Fluorescence emission spectra of dipyme solubilized by **AT 22-2** at two different concentrations in water. The sharper line corresponds to the spectrum shown in Figure 6c, and the noisier line to that of the same solution after dilution by a factor of 20 with water.[32]

can be solubilized in an aqueous solution of **AT 22-2**, and we obtain the spectrum shown in Figure 6c.

One of the attractive features of using dipyme as a probe of micellar properties is that it also reports on its location in the system. Because of the oxygen in the position β to the pyrene, the vibrational fine structure of the pyrene monomer fluorescence is much more sensitive to the polarity of its environment than in other 1-substituted pyrene derivatives. The I_1/I_3 ratio for dipyme solubilized in **AT 22-2** is equal to 1.28, similar to its value in 1,4-dioxane and slightly smaller than its value in SDS (1.38). These results establish the location of the dipyme probe as being within the core of micelles formed by the polymer, in an environment slightly more hydrophobic than that of its environment in SDS micelles.

In Figure 6c, we see that the monomer fluorescence intensity I_M (at 370−400 nm) of dipyme in the 1 wt % solution of **AT 22-2** is significantly enhanced, and the excimer emission intensity I_E (at wavelengths above 450 nm) is reduced, relative to that in other media. For the AT micelle we infer that the core microviscosity is much greater than that of an SDS micelle and even larger than that of bulk cyclohexanol ($\eta \approx 65$ cP). Thus we learn that the hydrophobic core of the micellar structures formed by HEUR polymers is much more rigid than that formed by normal surfactants. The IPDU group may play a role in promoting this rigidity.

Polymer Concentration Effects on Dipyme Fluorescence. When the concentration of polymer **22−2** is increased from 1.0 to 2.0 wt %, the macroscopic solution viscosity increases by nearly 2 orders of magnitude. Yet, the dipyme fluorescence spectrum does not change. When the 1.0 wt % AT solution of Figure 6c is diluted 20-fold with water, the macroscopic viscosity drops to essentially that of pure water ($\eta \approx 1.0$ cP), and we obtain the spectrum shown in Figure 7. While this spectrum is much noisier than that obtained at higher polymer concentrations, there is no significant change in the I_E/I_M ratio.[32]

Our experiments show that the spectrum of dipyme is essentially invariant with AT polymer concentration over the range of 0.01−2.0 wt %. This represents a broader range of concentrations than that over which aggregation numbers were determined. Both sets of results are consistent in that they lead to the conclusion that N_R and the local fluidity of the micellar core remain constant over a range of concentrations in which the macroscopic low-shear viscosity increases by more than 3 orders of magnitude.

The Micellar Dimension—The Hydrophobic Core. While recognizing the limitations of the detailed meaning of microfluidity and k_1, we can use these numbers in the context of the liquid drop model to estimate a first-order approximation of the size of the micellar cores formed in our system. Excimer formation is diffusion-controlled, and in bulk fluid media $k_{diff} = 4\pi N_A D\sigma$. Here D is the local diffusion coefficient of pyrene within the droplet, σ is the capture radius for excimer formation, and N_A is Avogadro's number. Within a liquid droplet of radius R,

$$k_1 = k_{diff}/N_A(4/3)\pi R^3 = 3D\sigma/R^3 \tag{7}$$

$$\frac{(k_1)_{SDS}}{(k_1)_{AT}} = \frac{D_{SDS}}{D_{AT}}\left(\frac{R_{AT}}{R_{SDS}}\right)^3 \tag{8}$$

For self-diffusion, $D = kT/\zeta$, where ζ is the microscopic friction coefficient. We make the assumption that intramolecular excimer formation in dipyme probes the same friction coefficient as bimolecular pyrene excimer formation. This allows us to equate the ratio of I_E/I_M values for dipyme to the ratio of D values shown in eq 8. Since the ratio $(I_E/I_M)_{SDS}/(I_E/I_M)_{AT} = 5.5$, we find that $R_{AT}/R_{SDS} = 1.2$. Note that problems with various assumptions made in this analysis are mitigated by the fact that one takes the cube root of the ratio determined in eq 8. The radius of the SDS micelle is approximately 1.6 nm. From this value, we estimate that the hydrophobic core size probed by pyrene excimer formation in **AT 22-2** is ca. 1.9 nm. We find it interesting that the AT micellar core is found to be larger than an SDS micelle, since the latter has a 3-fold larger aggregation number ($N_{R(SDS)} = 60$). Part of this effect is likely due to the longer alkyl chain, and part may be due to the isophorone unit connecting each end group to the PEO chain.

We can use the value of R_{AT} in conjunction with eq 7 to calculate a value for D. Since σ for pyrene excimer formation is approximately 1.0 nm,[33] we estimate the local diffusion coefficient for pyrene within the AT micellar core to be 7×10^{-8} cm^2 s^{-1}.

An alternative approach can be used to confirm the idea that the micelle core radius is on the order of 2 nm. We can use a mixture of donor and acceptor dyes as probe in the system. Simple derivatives of phenanthrene (donor) and anthracene (acceptor) have a critical Förster radius (R_0) of 2.3 nm. We found that the pair consisting of MePhe as the donor and MeAn as the acceptor have the desired degree of solubility in the micellar AT solutions.

Figure 8 shows the fluorescence spectra one obtains from the fluorescent probes with 0.5 wt % **AT 22-2** as the solvent and an excitation wavelength of 297 nm. Figure 8a shows the spectrum when the system contains 17 μM of MePhe. When the solution contains 24 μM of MeAn (Figure 8b), the emission intensity is weak because the absorbance of MeAn at 297 nm is very small. Figure 6c shows the spectrum when the solution contains 17 μM of the donor MePhe together with 24 μM of the acceptor MeAn. As a result of direct nonradiative energy transfer, the emission intensity of MePhe is reduced while that of MeAn is enhanced substantially.

If the micelle core were sufficiently rigid that no net diffusion of MePhe or MeAn occurred on the time scale of the MePhe fluorescence (53 ns), a much more detailed analysis of this experiment would be possible: one could use the theory of energy transfer in restricted dimensions to obtain the size of the core.[24,34] Chromophore diffusion occurs, and from the value of $D_{AT(Py)}$, we can calculate that a mutual displacement of about 15 Å (i.e., $(6Dt)^{1/2}$, with $t = 53$ ns) occurs during the MePhe lifetime. From a qualitative point of view, we can assert that the efficiency of energy transfer is sufficiently high that the core radius could not be much larger than R_0 (2.3 nm). On the other hand, if the radius were much smaller, the dye pair would be confined to such a small space that their proximity would lead to distortions in their excitation spectra. This is not observed.

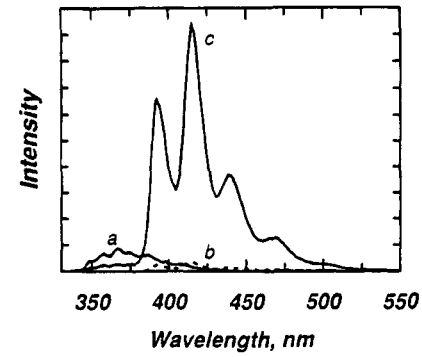

Figure 8. Fluorescence emission spectra of MePhe and MeAn solubilized in water by **AT 22-2** (0.5 wt %) upon excitation at 297 nm: (a) 17 μM MePhe; (b) 24 μM MeAn; (c) 17 μM MePhe + 24 μM MeAn.

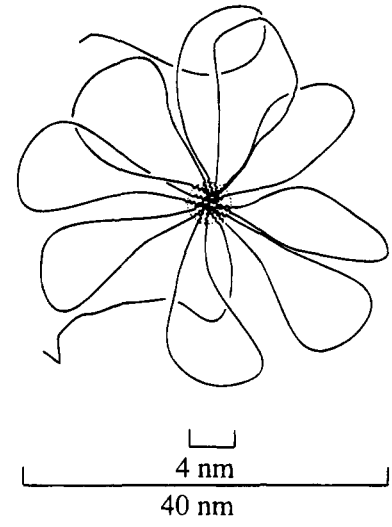

Figure 9. Drawing of the structure of a rosette-like micelle with a hydrophobic core and a corona comprised primarily of looped chains. To represent our sample, we show 10 polymers in the micelle and 18 chain ends making up the core. The 2 dangling chains represent the polymers with a hydrophobic group at only one end.

The Association Mechanism. Low-Concentration Regime. In a preliminary communication of some of the results reported here, we suggested a "microgel" model for the association structure of the HEUR polymers in solution.[14] An essential feature of this model is that over a broad range of polymer concentrations above the onset of association (a few ppm), the polymers exist in the form of rosette-like micelles. An aggregation number of 20, for polymers with hydrophobic groups on both ends, implies that on average 10 polymer chains come together to form a hydrophobic core containing the 20 $C_{16}H_{33}O$ end groups. In Figure 9 we show a picture of this type of structure in which two of the chains have dangling ends lacking a hydrophobic substituent.

Self-associated looped structures are controversial because a theoretical analysis by ten Brinke and Hadzi-

ioannou found excessive penalties of back-folding and loop formation in ABA triblock copolymer solutions with poorly solvated end blocks.[35] More recent theoretical and experimental work has challenged this conclusion and showed that in such triblocks under conditions of strong segregation micelle formation is possible; and if the segregation is weak, gel-like macrophase separation takes place.[36] Loops and rosettes are detected in the lattice chain simulations of Balazs et al.[18] Recent scattering experiments on PEO–PPO–PEO triblock copolymers in xylene and on PPO–PEO–PPO triblocks in water also indicate the formation of micelles with looped chain structures.[37]

What determines the onset of association? Annable et al.[9] studied HEUR polymers similar to **AT 22-2** with a series of *n*-alkyl end groups coupled to the PEO via IPDU. At 1.5 wt % concentration, they suggest that viscosity enhancement requires at least a C_6H_{13} hydrophobe. An insight into this issue is provided by a fluorescence decay study of a pyrene-end-capped PEO of $M_n = 8000$ in water at very low concentration (10^{-6} M).[38] Here the end groups were $PyCH_2O$, perhaps as hydrophobic as a C_8H_{17} chain. At this concentration, all polymer chains were molecularly dispersed. The authors showed that 7% of the molecules were cyclized, with the pyrene groups in proximity, and the other 93% had their chain ends free in solution. The extent of cyclization at this low concentration is enhanced if the PEO chain is shorter and diminished if it is longer, as one would expect for a negative free energy of binding in competition with an unfavorable entropy of cyclization.

The onset of association for micelles is determined by the free energy of the association process, which Annable et al. find from viscosity measurements to be 67 kJ/mol for the C_{16} chain. From temperature-dependent studies of the stress relaxation time, they find a corresponding binding enthalpy of 71 kJ/mol. These binding energies represent a balance between the association energy for incorporation of the hydrophobic group into the micelle and the free energy needed to stretch the PEO chains to allow them to pack into the micellar corona. The net binding energies are very strong, consistent with the onset of association at very low polymer concentrations. The concentration of free chain ends bearing hydrophobic groups will be very low. The only dangling ends permitted in such systems at concentrations above 0.05 wt % are those which, because of incomplete reaction during the polymer synthesis, lack hydrophobic end groups.

There is still no compelling evidence to indicate whether the onset of association in the ppm concentration region is sharp, as would be expected for a true critical micelle concentration (cmc) or whether the transition is gradual. Some experiments have detected a broad transition range. Recent experiments from J. François' laboratory in Strasbourg with model systems suggest a narrowing of the cmc transition.[39]

Returning to our system, we determined that in water at 22 °C, **AT 22-2** has an intrinsic viscosity $[\eta]$ of 1.1 dL/g. In terms of a hard sphere model and the now-known aggregation number, we calculate a rosette-micelle radius of 20 nm. Dynamic light scattering measurements in the range of 1 g/L concentration give a hydrodynamic radius R_H of 25 nm. Macdonald and co-workers[40] examined our samples, both **AT 22-2** and **Control 23-2**, by PGSE NMR over a wide range of concentrations. Based upon the extrapolated D_0 value, they calculate $R_H = 20$ nm for **AT 22-2**. For **Control 22-3** they find $R_H = 9.4$ nm, which agrees with the value anticipated from the results of Devanand and Selser[41] on PEO itself in water for a chain of that length. This supports the conclusion of a rosette-like micelle for **AT 22-2** in which the only dangling ends are due to the ca. 60% of the chains which contain a hydrophobe at only one end. The results of neutron scattering experiments by Ottewill et al. on the $C_{16}D_{33}O$ analogue of sample **AT 107** are consistent with our picture.[21]

Properties at Elevated Concentrations. Many authors have considered that the concentration range over which one observes the onset of the sharp increase in solution viscosity corresponds to the overlap concentration of the polymer chains in solution. They have attempted to estimate a value of c^* from the solution properties of PEO chains with the same chain length as the AT polymer. This is equivalent to assuming that the polymers remain unassociated below c^*.

The sharp rise in solution viscosity occurs in the concentration range of 0.1–0.8 wt %, far above the onset of polymer association. We have suggested that over a broad range of concentrations, the polymers exist in the form of rosette-like micelles. In this kind of system, the overlap concentration is determined by space-filling properties of the compact micelles. We can calculate the magnitude of c^* for **AT 22-2** as that in which spheres with a radius of 20 nm will fill space. This corresponds to a c^* of 1.7 wt %. At this concentration, there is already a pronounced increase in the solution viscosity.

According to Annable, micelle aggregation into localized networks should occur at lower concentrations.[9] These networks, which we called "microgels", are held together by bridging chains. Dilution of the solution is accompanied by breakup of these structures to smaller entities, accompanied by a transition of some of the bridging chains to looped configurations. Increasing the polymer concentration leads to larger aggregates of bridged micelles. In the Annable model, this transformation is entropically driven and gives rise to the strong initial concentration dependence of the viscosity and the viscoelastic modulus and relaxation time of the system.

The pictures Annable et al. draw for a series of bridged micelles are almost identical to those we proposed in our microgel model.[13,14] In these models, as the polymer concentration increases, the topology of the system evolves to form larger and larger objects composed of bridged micelles. If the global structures were compact in form and finite in size, one could think of them as microgels. If, on the other hand, they had a more open form, they would fit the picture of "superbridges" and "superloops" envisioned by Annable or the fractal-like structures suggested by Hansen.

Responses to Shear and to Changes in Concentration. We attempt to capture in Figure 10 the ideas described above. The graph presents rheological data (η vs oscillatory shear rate $\dot{\gamma}$) for our sample **AT 22-3** at a concentration of 1 wt %. At this concentration, a pronounced shear thickening occurs in the range of $\dot{\gamma} \approx$ 40 Hz. At higher shear rates, shear thinning becomes dominant. For increased polymer concentrations, the low-shear viscosity is enhanced, the extent of shear thickening becomes less pronounced, and over the same range of $\dot{\gamma}$, the shear thinning becomes even more precipitous.

In Figure 10 we superpose over regions of the data our picture of the structure of the system. At low shear

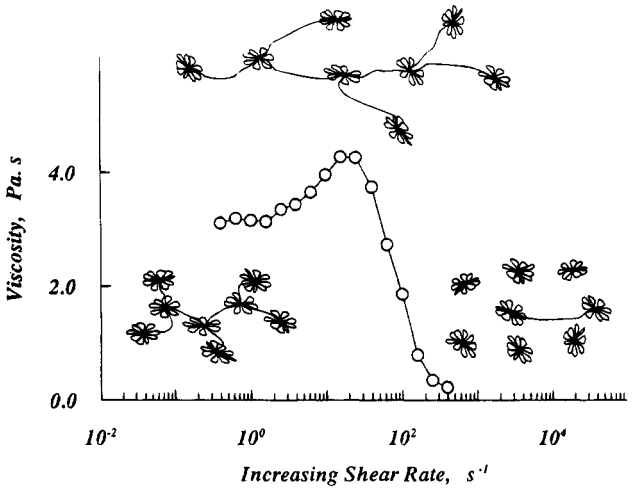

Figure 10. Plot of viscosity vs shear rate measured at 22 °C for **AT 22-3** at 1.0 wt % concentration. Shown on the left is a drawing depicting a structure that might form at this concentration through association of 8 micelles. For simplicity, the dangling chain ends shown in Figure 9 are not drawn here. At higher shear rates, this structure is stretched, and shear thinning occurs when the structure fragments and the polymers rearrange. A key feature of the model is that the mean aggregation number of chain ends in the micellar core remains at 18 throughout the range of shear rates.

rates, the system is comprised of clusters of micelles held together by bridging chains. The size of these clusters depends upon the polymer concentration. Here we draw a cluster made up of eight micelles. In the shear-thickening region, the structure is stretched, accompanied by deformation of the conformations of the bridging chains. Increasing the shear rate increases the stress on such structures, and once a critical force is exceeded, fragmentation occurs. Fragmentation involves pull-out of one end of a bridging chain. It exits from its micelle and loops back to join its other end in an adjacent micelle. A prediction of this model is that shear or extensional stresses which lead to shear thinning also accelerate the exit rate of the hydrophobes of bridging chains from their micelles.

This model receives strong support from fluorescence experiments carried out on HEUR systems under shear[16] or extensional flow.[12] These experiments show *no changes* in signal under conditions where both shear thickening and strong shear or extensional thinning are observed, results which require that the average size and structure of the micellar core be conserved throughout the transition region.

It is useful at this point to recall the model for the association structure suggested by Maechling-Strasser[15] based upon light scattering measurements to determine the apparent M_w of the system as a function of concentration. They proposed an *open association* model in which the fundamental building blocks were unassociated polymer chains. In our model, individual polymer chains associate to form micelles of a well-defined structure (i.e., *closed association*), but these micelles undergo secondary association to form clusters. Since the size of the structure formed increases with polymer concentration, cluster formation follows an *open association* process. Thus one might find similarities between our model and that of Maechling-Strasser, with the key difference that in our model the fundamental building blocks of the associated structure are the rosette-like micelles.

The dynamic light scattering (DLS) and pulsed-gradient spin–echo NMR experiments of Nyström and Hansen in the enhanced-viscosity concentration regime suggest a fractal-like structure with relaxation processes that slow down as the polymer concentration is increased.[20b] One would very much like to know what kinds of motion give rise to these relaxation processes. At very high polymer concentrations, polymer diffusion might involve a "slinky-toy" type motion in which the chains undergo a series of loop–bridge, bridge–bridge, and bridge–loop steps. If the Annable model is correct, then the step time for this motion will also be the time needed for the hydrophobic group to exit from the micellar core.

Summary

We have examined four polymers with a PEO backbone and $C_{16}H_{33}O$ end groups attached to the polymer via IPDU urethane linkages. These polymers associate in water, beginning at very low concentrations (a few ppm) to form micelle-like objects. Here we use pyrene as a fluorescent probe to establish that, over a series of polymer concentrations, ca. 20 chain ends are incorporated into each aggregate. Experiments with a second probe, dipyme, indicate that the aggregation number remains constant over a very broad range of polymer concentrations and over a wide range of flow conditions, representing orders of magnitude changes in solution viscosity. From these results, a model is presented involving closed association of the end groups to form micelles as the primary aggregate, and at higher concentrations, secondary aggregates via an open association process. The secondary aggregates are held together via bridging chains. Dilution and shear lead to a decrease of the solution viscosity via breakup of the secondary aggregates, accompanied by a bridge-to-loop transition of the bridging chains. This process conserves the number of hydrophobic groups in each primary micelle.

Acknowledgment. The authors thank NSERC Canada, Union Carbide, and Aqualon for their support of this research and Dr. S. Menchen (Applied Biosystems) for the sample **AT 67-3**. We also thank Dr. Lin Li for the rheological data incorporated into Figure 10.

References and Notes

(1) Current address: Department of Chemistry, University of Pennsylvania, Philadelphia, PA.
(2) (a) *Water-Soluble Polymers*; Glass, J. E., Ed.; Advances in Chemistry 213; American Chemical Society: Washington, DC, 1986. (b) *Polymers in Aqueous Media*; Glass, J. E., Ed.; Advances in Chemistry 223; American Chemical Society: Washington, DC, 1989. (c) *Polymers as Rheology Modifiers*; Schulz, D. N., Glass, J. E., Eds.; ACS Symposium Series 462; American Chemical Society: Washington, DC, 1991.
(3) (a) Jenkins, R. D. Ph.D. Thesis, Lehigh University, Bethlehem, PA, 1990. (b) Jenkins, R. D.; Silebi, C. A.; El-Aasser, M. S. *Polym. Mater. Sci. Eng.* **1989**, *61*, 629. (c) Jenkins, R. D.; Silebi, C. A.; El-Aasser, M. S. In *Advances in Emulsion Polymerization and Latex Technology: 21st Annual Short Course*; El-Aasser, M. S., Ed.; Lehigh University, June 1990, Chapter 17.
(4) (a) Windermuth, E.; Berlenbach, W. (Bayer) German Patent 1069735, 1964. (b) Fikentscher, R.; Oppenländer, K.; Müller, R. German Patent 2054885, 1972. (c) Singer, W.; Tenneck, N. J.; Driscoll, A. E. U.S. Patent 3770684, 1973. (d) Emmons, W. D.; Stevens, T. E. (Rohm and Haas) U.S. Patent 4079028, 1978. (e) Emmons, W. D.; Stevens, T. E. (Rohm and Haas) U.S. Patent 4155892, 1979. (f) Hoy, K. L.; Hoy, R. C. (Union Carbide), U.S. Patent Appl. 388202, 1982; Eur. Pat. Appl. EP96882, 1983. (g) Tetenbaum, M. T.; Crowley, B. C. (NL Industries), U.S. Patent 4499233, 1985.

(5) (a) Glass, J. E.; Fernando, R. H.; England-Jongewaard, S. K.; Brown, R. G. *JOCCA* **1984**, *10*, 256. (b) Schaller, E. J.; Sperry, P. R. In *Handbook of Coatings Additives*; Calbo, L. J., Ed.; Marcel Dekker: New York, 1992; Vol. II, Chapter 4. (c) Howard, P. R.; Leasure, E. L.; Rosier, S. T.; Schaller, E. J. *J. Coat. Technol.* **1992**, *64*, 87.
(6) Ballard, M. J.; Buscall, R.; Waite, F. A. *Polymer* **1988**, *29*, 1287.
(7) (a) Fonnum, G. Ph.D. Thesis, University of Trondheim, Norway, 1989. (b) Lundberg, D. J. Ph.D. Thesis, North Dakota State University, Fargo, ND, 1990.
(8) Fonnum, G.; Bakke, J.; Hansen, F. K. *Colloid Polym. Sci.* **1993**, *271*, 380.
(9) Annable, T.; Buscall, R.; Ettelaie, R.; Whittlestone, D. *J. Rheol.* **1993**, *37*, 695.
(10) Huldén, M. *Colloids Surf. A* **1994**, *82*, 263.
(11) Wang, Y.; Winnik, M. A. *Langmuir* **1990**, *6*, 1437.
(12) Vlahiotis, D. Ph.D. Thesis, University of Toronto, Toronto, Canada, 1992.
(13) Yekta, A.; Duhamel, J.; Brochard, P.; Adiwidjaja, H.; Winnik, M. A. *Macromolecules* **1993**, *26*, 1829.
(14) Yekta, A.; Duhamel, J.; Adiwidjaja, H.; Brochard, P.; Winnik, M. A. *Langmuir* **1993**, *9*, 881.
(15) (a) Maechling-Strasser, C.; François, J.; Clouet, F.; Tripette, C. *Polymer* **1992**, *33*, 627. (b) Maechling-Strasser, C.; Clouet, F.; François, J. *Polymer* **1992**, *33*, 1021. (c) François, J. *Prog. Org. Coat.* **1994**, *24*, 67.
(16) Richey, B.; Kirk, A. B.; Eisenhart, E. K.; Fitzwater, S.; Hook, J. *J. Coat. Technol.* **1991**, *63*, 31.
(17) Walderhaug, H.; Hansen, F. K.; Abrahamsén, S.; Persson, K.; Stilbs, P. *J. Phys. Chem.* **1993**, *97*, 8336.
(18) Balazs, A. C.; Hu, J. Y.; Lentvorski, A. P. *Phys. Rev. A* **1990**, *41*, 2109.
(19) Tanaka, F.; Edwards, S. F. *J. Non-Newtonian Fluid Mech.* **1992**, *43*, Part I, 247–271; Part II, 273–288; Part III, 289–309.
(20) (a) Persson, K.; Abrahmsén, S.; Stilbs, P.; Hansen, F. K.; Walderhaug, H. *Colloid Polym. Sci.* **1992**, *270*, 465. (b) Nyström, B.; Walderhaug, H.; Hansen, F. K. *J. Phys. Chem.* **1993**, *97*, 7743. (c) Ngai, K. L.; Rajagopal, A. K.; Teitler, S. *J. Chem. Phys.* **1988**, *88*, 5086.
(21) Ottewill, R. H. Private communications.
(22) (a) Georgescauld, D.; Desmasèz, R.; Lapouyade, R.; Babeau, A.; Richard, H.; Winnik, M. A. *Photochem. Photobiol.* **1980**, *31*, 539. (b) Winnik, F. M.; Winnik, M. A.; Ringsdorf, H.; Venzmer, J. *J. Phys. Chem.* **1991**, *95*, 2583. (c) Yekta, A.; Kanagalingam, S.; Xu, B.; Nivaggioli, T.; Winnik, M. A. In *Hydrophilic Polymers: Performance with Environmental Acceptance*; Glass, J. E., Ed.; Advances in Chemistry Series; American Chemical Society: Washington, DC, 1994.
(23) (a) Glass, J. E.; Kaczmarski, J. P. *Polym. Mater. Sci. Eng.* **1991**, *65*, 175. (b) Mast, A. P.; Prud'homme, R. K.; Glass, J. E. *Langmuir* **1993**, *9*, 708. (c) Kaczmarski, J. P.; Glass, J. E. *Macromolecules* **1993**, *26*, 5149.
(24) Duhamel, J.; Yekta, A.; Ni, S.; Skaykin, Y.; Winnik, M. A. *Macromolecules* **1993**, *26*, 62555.
(25) (a) Yekta, A.; Aikawa, M.; Turro, N. J. *Chem. Phys. Lett.* **1979**, *63*, 543. (b) Warr, G. G.; Grieser, F. *J. Chem. Soc., Faraday Trans. 1* **1986**, *82*, 1813.
(26) NMR analysis of *unpurified* samples gives misleading results because such samples contain significant amounts of $C_{16}H_{33}$ groups not attached to the polymer.
(27) A particularly apt comparison is with data on micelles of nonionic surfactants and mixtures of nonionic surfactants. (a) Abe, M.; Uchiyama, H.; Yamaguchi, T.; Suzuki, T.; Ogino, K. *Langmuir* **1992**, *8*, 2147. (b) Alami, E.; Kamenka, N.; Raharimihamina, A.; Zana, R. *J. Colloid Interface Sci.* **1993**, *158*, 342.
(28) (a) Atik, S. S.; Nam, M.; Singer, L. A. *Chem. Phys. Lett.* **1979**, *67*, 75. (b) Lianos, P.; Lang, J.; Strazielle, C.; Zana, R. *J. Phys. Chem.* **1982**, *86*, 1019. (c) Malliaris, A.; Paleos, C. M. *J. Colloid Interface Sci.* **1984**, *101*, 364. (d) Duhamel, J.; Yekta, A.; Winnik, M. A. *J. Phys. Chem.* **1993**, *97*, 2759.
(29) Birks, J. B. *Photophysics of Aromatic Molecules*; Wiley-Interscience: New York, 1971.
(30) (a) Kubota, Y.; Miura, M. *Bull. Chem. Soc. Jpn.* **1973**, *46*, 100. (b) Nakashima, K.; Anzai, T.; Fujimoto, Y. *Langmuir* **1994**, *10*, 658.
(31) (a) Zachariasse, K. A.; Vaz, W. L. C.; Sotomayor, C.; Kühnle, W. *Biochim. Biophys. Acta* **1982**, *688*, 323. (b) Turro, N. J.; Aikawa, M.; Yekta, A. *J. Am. Chem. Soc.* **1979**, *101*, 772. (c) Reference 28b.
(32) Some associated polymer networks have very slow relaxation times. This seems not to be a factor here, since the spectrum shown in Figure 7 remains unchanged after the sample is allowed to age in the dark for 1 week at room temperature.
(33) (a) Transient-effects kinetics have been used extensively to probe the details of pyrene excimer formation. The effective capture radius σ is not a true constant and depends on the type of solvent and also on the pyrene diffusion coefficient D (i.e., the local viscosity). Experimentally determined values of σ lie in the range of 0.4–1.4 nm, with the higher values observed at lower values of D. (b) Martinho, J. M. G.; Winnik, M. A. *J. Phys. Chem.* **1987**, *91*, 3640. (c) Martinho, J. M. G.; Sienicki, K.; Blue, D.; Winnik, M. A. *J. Am. Chem. Soc.* **1988**, *110*, 7773. (d) Martinho, J. M. G.; Tencer, M.; Campos, M.; Winnik, M. A. *Macromolecules* **1989**, *22*, 322. (e) Xu, R.; Winnik, M. A. *J. Photochem. Photobiol. A: Chem.* **1991**, *57*, 351.
(34) (a) Klafter, J.; Blumen, A. *J. Chem. Phys.* **1984**, *80*, 875. (b) Drake, J. M.; Klafter, J.; Levitz, P. *Science* **1991**, *251*, 1574.
(35) ten Brinke, G.; Hadziioannou, G. *Macromolecules* **1987**, *20*, 486.
(36) (a) Balsara, N. P.; Tirrell, M.; Lodge, T. P. *Macromolecules* **1991**, *24*, 1975. (b) Wang, Y.; Mattice, W. L.; Napper, D. H. *Macromolecules* **1992**, *25*, 4073.
(37) Zhou, Z.; Chu, B. *Macromolecules* **1994**, *27*, 2025.
(38) Duhamel, J.; Yekta, A.; Hu, Y. Z.; Winnik, M. A. *Macromolecules* **1992**, *25*, 7024.
(39) Binana-Limbele, W.; Clouet, F.; François, J. *Colloid Polym. Sci.* **1993**, *271*, 748.
(40) Macdonald, P. M.; Uemura, Y.; Dyke, L. In *Hydrophilic Polymers: Performance with Environmental Acceptance*; Glass, J. E., Ed.; Advances in Chemistry Series; American Chemical Society: Washington, DC, 1994.
(41) Devanand, K.; Selser, J. C. *Macromolecules* **1991**, *24*, 5943.

MA941185V